ISSN 1674-1056
http://cpb.iphy.ac.cn
http://iopscience.iop.org/cpb
中国物理 B
Chinese Physics
中国物理 Chinese Physics B

Dynamically tunable optical properties in graphene-based plasmon-induced transparency metamaterials

Wei Jia(贾微), Pei-Wen Ren(任佩雯), Yu-Chen Tian(田雨宸), Chun-Zhen Fan(范春珍)

Citation: Chin. Phys. B . 2019, 28(2): 026102. **doi:** 10.1088/1674-1056/28/2/026102
Journal homepage: http://cpb.iphy.ac.cn; http://iopscience.iop.org/cpb

What follows is a list of articles you may be interested in

Charge noise acting on graphene double quantum dots in circuit quantum electrodynamics architecture

Yan Li(李炎), Shu-Xiao Li(李舒啸), Hai-Ou Li(李海欧)dag, Guang-Wei Deng(邓光伟), Gang Cao(曹刚), Ming Xiao(肖明), Guo-Ping Guo(郭国平)

Chin. Phys. B . 2018, 27(7): 076105. **doi:** 10.1088/1674-1056/27/7/076105

Preparation of graphene oxides with different sheet sizes by temperature control

Zhe Qian(钱哲), Liang Chen(陈亮), De-Yuan Li(李德远), Bing-Quan Peng(彭兵权), Guo-Sheng Shi(石国升), Gang Xu(徐刚), Hai-Ping Fang(方海平), Ming-Hong Wu(吴明红)

Chin. Phys. B . 2017, 26(10): 106101. **doi:** 10.1088/1674-1056/26/10/106101

Controllable preparation of vertically standing graphene sheets and their wettability and supercapacitive properties

Hai-Tao Zhou(周海涛), Ning Yu(喻宁), Fei Zou(邹飞), Zhao-Hui Yao(姚朝晖), Ge Gao(高歌), Cheng-Min Shen(申承民)

Chin. Phys. B . 2016, 25(9): 096106. **doi:** 10.1088/1674-1056/25/9/096106

Impurity effects on electrical conductivity of doped bilayer graphene in the presence of a bias voltage

E Lotfi, H Rezania, B Arghavaninia, M Yarmohammadi

Chin. Phys. B . 2016, 25(7): 076102. **doi:** 10.1088/1674-1056/25/7/076102

Finite temperature effect on mechanical properties of graphene sheets with various grain boundaries

Yong Ge(葛勇), Hong-Xiang Sun(孙宏祥), Yi-Jun Guan(管义钧), Gan-He Zeng(曾赣鹤)

Chin. Phys. B . 2016, 25(6): 066104. **doi:** 10.1088/1674-1056/25/6/066104

Dynamically tunable optical properties in graphene-based plasmon-induced transparency metamaterials*

Wei Jia(贾微), Pei-Wen Ren(任佩雯), Yu-Chen Tian(田雨宸), and Chun-Zhen Fan(范春珍)†

School of Physical Science and Engineering, Zhengzhou University, Zhengzhou 450001, *China*

(Received 9 September 2018; revised manuscript received 9 November 2018; published online 10 January 2019)

A graphene-based metamaterial for THz plasmon induced transparency (PIT) is presented and numerically studied in this paper, which consists of two horizontal graphene strips attached to a continuous vertical wire separately. The calculated surface current distributions demonstrate that the distinct PIT window results from the near-field coupling of two bright modes. To explore the physical mechanism of PIT effect, we employ the coupled Lorentz oscillator model. The transmission spectra obtained with this model fits well with the simulation results. The performance of the PIT system can be controlled through the geometry parameters of graphene strips. Moreover, the transparency window can be dynamically tuned by varying the Fermi energy and the carrier mobility of the graphene strips. The slow light effect is also explored in our proposed structure and it can achieve 1.25 ps when Fermi energy is 1.3 eV. Finally, the position of the transmission window with the variation of the nearby medium refractive index is examined. Such a proposed graphene-based PIT system may have great potential applications in photonic devices.

Keywords: plasmon-induced transparency, graphene, tunable

PACS: 61.48.Gh, 42.79.Hp, 78.67.Pt, 42.50.Gy **DOI:** 10.1088/1674-1056/28/2/026102

1. Introduction

Electromagnetically induced transparency (EIT) occurring in laser-activated atomic systems has attracted much attention since the first experimental demonstration in 1991.[1–3] It is a quantum interference effect between the atomic level and the excitation pathways, which results in a narrow transmission window due to electromagnetic interference coupling. The EIT effect dramatically modifies the optical dispersion properties of the medium, namely, it can slow down photons and enhance nonlinear characteristics. Harsh experimental requirements for the ultra-low temperature and rare atoms slow down its development. While metamaterials can mimic this EIT effect due to coupling between plasmonic resonances of meta-atoms, resulting in the so-called plasmon-induced transparency (PIT).[4,5] The unique properties of the PIT has wide applications in sensor,[6–9] optical storage,[10,11] optical switch,[12,13] *etc*. At present, there are usually two ways to implement the PIT phenomenon, including the bright–bright mode coupling[14,15] and the bright–dark mode coupling.[16–18] The first way is based on the weak hybridization between two bright modes, and the second way is achieved by the destructive interference between dark mode and bright mode. Zhu *et al.* proposed a simple structure of two parallel coupling coplanar metallic strips to realize obvious PIT behavior.[19] Zhang *et al.* designed a typical PIT structure, which consists of three metal strips and can be used as a building block to construct a slow light plasmonic metamaterial.[20] Liu *et al.* provided an optical metamaterial structure that comprises a gold bar stacked above two symmetric gold wires to obtain the PIT effect.[21] Tian *et al.* investigated the PIT effect in a three-dimensional (3D) plasmonic metamaterial composed of three identical rings.[16] However, as far as metals are concerned, it is hardly tunable without refabrication of the structures and novel metals usually exhibit large Ohmic losses, which restricts their application in optical processing devices.

Recently, graphene, a two-dimensional (2D) conductive material which is arranged by a planar sheet of carbon atoms,[22] has attracted a lot of attention and has been used to design the PIT devices due to its excellent optical properties, unique tunability, long plasmon lifetime and high degree of electromagnetic confinement.[23–28] Fu *et al.* have proposed and numerically investigated two parallel-coupled coplanar graphene nanostrips to realize the PIT effect.[14] Shang *et al.* have designed a tunable PIT structure which consists of three graphene strips.[17] Sun *et al.* have proposed a tunable multispectral PIT device based on periodically patterned graphene double layers separated by a dielectric layer.[29] The surface plasmon resonance of graphene has a very high correlation with the Fermi energy which can be controlled via electrostatic gating or chemical doping.[30]

In this paper, a simple PIT structure which is composed of two coupled horizontal graphene strips attached to continuous vertical wire is proposed and numerically studied. Since the two resonators can directly interact with the incident light in the THz region, they serve as the bright modes. The weak hy-

*Project supported by the Key Science and Technology Research Project of Henan Province, China (Grant Nos. 162102210164 and 1721023100107) and the Natural Science Foundation of Henan Educational Committee, China (Grant No. 17A140002).

†Corresponding author. E-mail: chunzhen@zzu.edu.cn

© 2019 Chinese Physical Society and IOP Publishing Ltd

bridization between the two bright modes as a function of frequency detuning gives rise to the PIT optical response in the THz region. A Lorentz oscillator model has been employed to verify the transmission spectrum. In addition to the geometry parameters, the PIT response can also be modulated actively by the Fermi energy E_F and the carrier mobility μ of the graphene structure. The group delay and the sensitivity of our proposed structure are also investigated. Such a simple graphene-based PIT metamaterial offers potential applications in THz plasmonic devices such as tunable sensors, switchers, and filters.

2. Structure design and simulation method

The designed graphene-based PIT metamaterial structure is shown in Fig. 1. The unit cell consists of two parallel strip resonators attached to a continuous vertical wire, separately. Figure 1(a) is the unit cell of a graphene nanostructure on a substrate with a refractive index 1.5. Figure 1(b) represents the overall schematic diagram of the structure. The unit cell of monolayer graphene periodically arranges on the substrate and its thickness is 1 nm. Let L_1 and L_2 represent the length of two horizontal strips with a vertical spacing of d in between. The width of the continuous vertical antenna and horizontal strip attached to it are both denoted by w. The specific geometrical parameters are detailed in Fig. 1. The periodicity is 6.6 μm in each of x and y directions. The plane wave polarizing along the x direction is normally incident to the structure surface along the z direction. Both the transmission spectra and the field distribution are calculated by using COMSOL Multiphysics, which is commercial software based on the finite element method. The computation domain consists of only a unit cell with the perfectly matched layer applied to the boundary along the propagation direction (z axis) and periodic conditions imposed on the four lateral boundaries in the x-axis and y-axis directions.

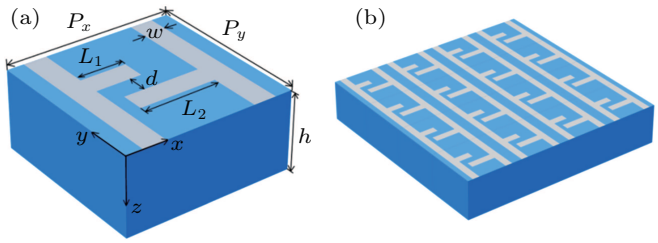


Fig. 1. Schematic view of graphene-based PIT metamaterial on a substrate with refractive index 1.5, showing (a) unit cell structure, (b) overall structure of proposed PIT metamaterial. Geometry parameters are $L_1 = 1.8$ μm, $L_2 = 3.0$ μm, $d = 0.8$ μm, $w = 0.9$ μm, $h = 3$ μm, and Fermi energy is 1.0 eV. Thickness of graphene is 1 nm. Periodicity is 6.6 μm in each of x and y directions. Grey region refers to graphene layer and blue region represents dielectric substrate.

In the simulations, graphene is modeled as a conductive surface, using the transition boundary condition.[31,32] The conductivity of graphene can be derived within the random-phase approximation (RPA) in the local limit[33]

$$\begin{aligned}\sigma(\omega) = {} & \frac{2e^2 k_B T}{\pi\hbar^2}\frac{\mathrm{i}}{\omega+\mathrm{i}\tau^{-1}}\ln\left[2\cosh\left(\frac{E_F}{2k_B T}\right)\right] \\ & + \frac{e^2}{4\hbar}\left[\frac{1}{2}+\frac{1}{\pi}\arctan\left(\frac{\hbar\omega-2E_F}{2k_B T}\right)\right. \\ & \left. - \frac{\mathrm{i}}{2\pi}\ln\frac{(\hbar\omega+2E_F)^2}{(\hbar\omega-2E_F)+4(k_B T)^2}\right]. \end{aligned} \tag{1}$$

Here k_B is the Boltzmann constant, T is the temperature, ω is the angular frequency, τ is the carrier relaxation lifetime, E_F is the Fermi energy of graphene, e is the charge of an electron, and $\hbar$ is the reduced Planck's constant. In the simulation, our method mainly focuses on the material effect in 2D flat surface while ignoring that in out-of-plane direction. As can be seen from Eq. (1), the conductivity of graphene includes interband and intraband transition contribution. In the terahertz frequency domain ($E_F \gg \hbar\omega$), only the intraband transition dominates due to the Pauli exclusion principle, and the condition of $E_F \gg k_B T$ is satisfied at room temperature. Thus, the in-plane conductivity of the graphene can be represented by a Drude model as follows:[34]

$$\sigma(\omega) = \frac{e^2 E_F}{\pi\hbar^2}\frac{\mathrm{i}}{\omega+\mathrm{i}\tau^{-1}}, \tag{2}$$

where τ is the intrinsic relaxation time, and equals $\mu E_F/ev_F^2$, with $v_F = c/300$ being the Fermi velocity and $\mu = 10^4$ cm$^2\cdot$V$^{-1}\cdot$s^{-1} being the measured DC mobility.[35] Then we can obtain the permittivity of graphene from the following equation:

$$\varepsilon = 1 + \frac{\mathrm{i}\sigma(\omega)}{\varepsilon_0 t\omega}, \tag{3}$$

where ε_0 is the permittivity of a vacuum. $t = 1$ nm is the thickness of monolayer graphene film which can be obtained through the chemical vapor deposition method.[36]

3. Results and discussion

In order to demonstrate the PIT phenomenon, we separately calculate the transmission spectra of single graphene strip attached to a continuous vertical wire with $L_1 = 1.8$ μm (black line), $L_2 = 3.0$ μm (red line) and the combination of two structures (blue line) in Fig. 2. The Fermi energy and the spacing between two horizontal strips attached to a continuous vertical wire remain the same in all simulations. The short graphene strip attached to the continuous vertical wire shows a resonance at 4.36 THz and the long strip attached to the continuous vertical wire exhibits a resonance at 3.41 THz. This resonant dip arises from direct coupling with the incident light. When two resonators are integrated together to construct an integrated structure, a distinct transparency window with an amplitude of 92.9% is obtained at 4.02 THz. The destructive

interference resulting from near-field coupling of two bright modes induces a distinct transparency window.[37] Compared with the resonant frequencies of two isolated resonators, two resonant dips of the PIT structure show a slight blue shift due to the coupling effect between each other.

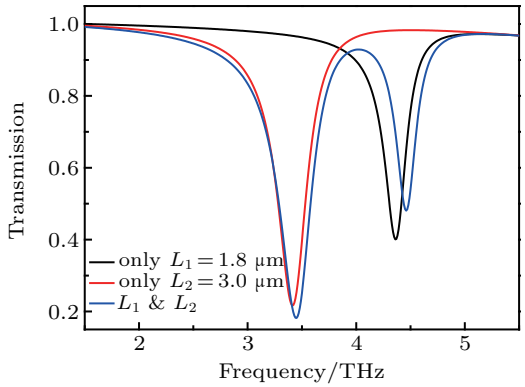


Fig. 2. Transmission spectra of single graphene horizontal strip attached to continuous vertical wire only with short strip $L_1 = 1.8$ μm (black line), long strip $L_2 = 3.0$ μm (red line), and combined structure (blue line) with $d = 0.8$ μm, $w = 0.9$ μm, $h = 3$ μm, and $E_F = 1.0$ eV.

To fully dig out the physical origin of the observed PIT phenomenon, the distribution of normalized electric field and surface current corresponding to the two transmission dips (3.45 THz and 4.46 THz) and the transmission peak (4.02 THz) are shown in Fig. 3. It can be clearly observed that the electric field is mainly distributed on the horizontal graphene stripe L_2 at the 3.45 THz in Fig. 3(a), which means that only the long strip of L_2 interacts with the incident light and the short strip of L_1 hardly interacts with the incident light. It is also found that the directions of the induced current in the two horizontal graphene strips are the same and they are in phase, similar to the dipole oscillation. Similarly, only the short strip of L_1 is excited and the long graphene strip of L_2 is excited very weakly at the resonant frequency 4.46 THz in Fig. 3(c). For the transparency window at 4.02 THz, the electric field is evenly distributed on the two horizontally placed graphene strips, which means that both resonators undergo strong interaction with the incident light as shown in Fig. 3(b). At this point, the directions of the induced current in two graphene strips are opposite, and they are in the opposite phase. Namely, a quadrupole oscillation is excited at the transparency peak due to the hybridization coupling between bright modes.[15] As a result, the destructive interference resulting from near-field coupling of two bright modes induces a distinct transparency window.

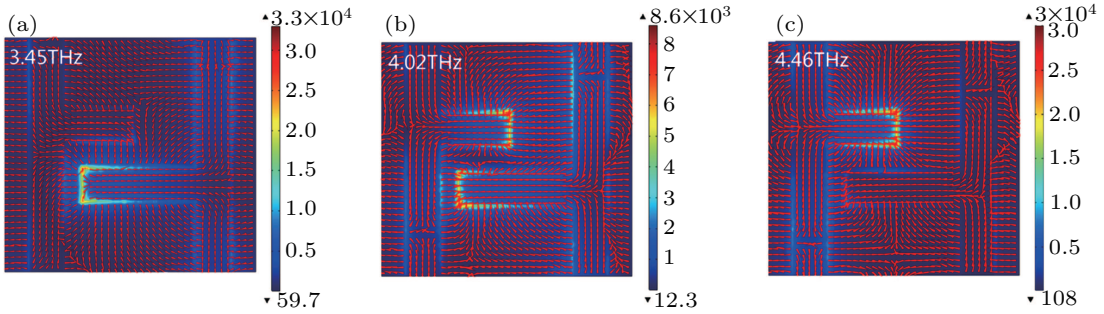


Fig. 3. Normalized electric field distributions and surface current distributions (red arrows) at two transmission dips and the transparency window at frequencies: (a) 3.45 THz, (b) 4.02 THz, and (c) 4.46 THz.

In order to better explain the physical mechanism of the proposed PIT structure, we adopt the three-level plasmonic system to analyze the calculated results.[38] The incident electromagnetic field is defined as $\tilde{E}\mathrm{e}^{\mathrm{i}\omega t}$, two bright modes can be described as $|B_1\rangle = \tilde{B}_1(\omega)\mathrm{e}^{\mathrm{i}\omega t}$ and $|B_2\rangle = \tilde{B}_2(\omega)\mathrm{e}^{\mathrm{i}\omega t}$ respectively. According to the coupled Lorentz oscillator model,[39–41] the field amplitude of the two bright modes can be expressed as

$$(\omega - \omega_1 + \mathrm{i}\gamma_1)\tilde{B}_1 + \kappa\tilde{B}_2 = g_1\tilde{E}, \tag{4}$$

$$(\omega - \omega_2 + \mathrm{i}\gamma_2)\tilde{B}_2 + \kappa\tilde{B}_1 = g_2\tilde{E}, \tag{5}$$

where ω_1, ω_2, and γ_1, γ_2 represent the resonance frequency and the damping factors of the two bright modes, respectively, ω is the incident frequency, κ is the coupling coefficient between two resonators, g_1 is the geometrical parameter describing the coupling strength of the first bright mode with the incident field, and g_2 is the geometry parameter depicting the coupling strength of the second bright mode with the incident field. By solving Eq. (4), the complex amplitude of the first bright mode can be derived as

$$\tilde{B}_1 = \frac{g_1\tilde{E}(\omega - \omega_2 + \mathrm{i}\gamma_2) - g_2\tilde{E}\kappa}{(\omega - \omega_1 + \mathrm{i}\gamma_1)(\omega - \omega_2 + \mathrm{i}\gamma_2) - \kappa^2}. \tag{6}$$

Then, the transmission of the proposed PIT device can be deduced as[38]

$$T(\omega) = 1 - \left|\frac{\tilde{B}_1}{\tilde{E}}\right|^2. \tag{7}$$

With the help of Eq. (7), we theoretically calculate the transmission spectrum of our proposed PIT structure in Fig. 4. It can be found that the simulation result fits well with the coupled Lorentz oscillator model with $\omega_1 = 4.46$ THz, $\omega_2 = 3.45$ THz, $\gamma_1 = 0.12$, $\gamma_2 = 0.19$, $g_1 = 0.24$, $g_2 = 2.8$, and $\kappa = 0.06$.

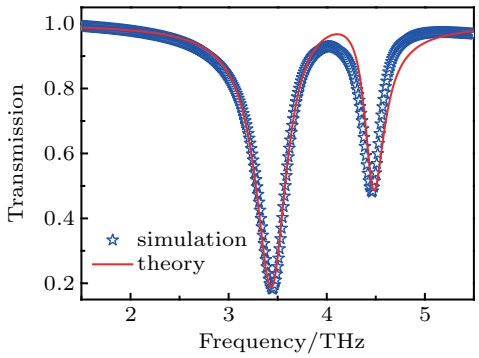


Fig. 4. Comparison between transmission spectra obtained from simulation and coupled Lorentz oscillator model theory with $L_1 = 1.8$ μm, $L_2 = 3.0$ μm, $d = 0.8$ μm, $w = 0.9$ μm, $h = 3$ μm, and $E_F = 1.0$ eV.

In the following, we numerically investigate the spectral response of the graphene nanostrips with different values of L_1 (keep L_2 as constant) and different values of L_2 (keep L_1 constant) with $d = 0.8$ μm, $E_F = 1.0$ eV in Fig. 5. It can be observed that the transparency peak shifts to the low frequency region and its strength diminishes with length L_1 increasing in Fig. 5(a). Similarly, when length L_2 increases, the transparency peak has a red shift in Fig. 5(b). For a fixed lateral displacement d, as the length difference between L_1 and L_2 decreases, the distance between the central axes of the two graphene strips decreases correspondingly. Namely, the coupling strength is enhanced between these two strips, which causes a strong coupling resonance to appear.

It should be particularly emphasized that the conductivity of graphene depends on its Fermi energy to a large extent.[42–44] By tuning the Fermi energy, the electron density in graphene is changed, resulting in the variation of the resonant frequency of graphene plasmonic nanostructures.[14] It can be observed that the transmission peak frequency is 4.02 THz when $E_F = 1.0$ eV in Fig. 6(a). With the increase of Fermi energy, the transmission peak frequency also gradually increases. When the Fermi energy is 1.3 eV, the transmission peak resonance frequency reaches a value of 4.45 THz. Namely, the transmission spectrum exhibits a significant blue shift with the increase of the Fermi energy. Such a blue shift can be explained through the relationship $f \propto \sqrt{E_F}$[34] The dispersion loss of the surface plasmons of graphene decreases as Fermi energy increases. Keeping the Fermi energy of the long graphene strip equal to 1.0 eV and only increasing the Fermi energy of the short graphene strip from 1.0 eV to 1.3 eV, it can be clearly seen from Fig. 6(b) that the high energy dip shows a significant blue shift, and the low energy dip is almost unchanged. Similarity, the increase of the Fermi energy of the long nanostrips results in the blue shift of its resonant dip with window in Fig. 6(c) narrowing, which can be used in optical filter.

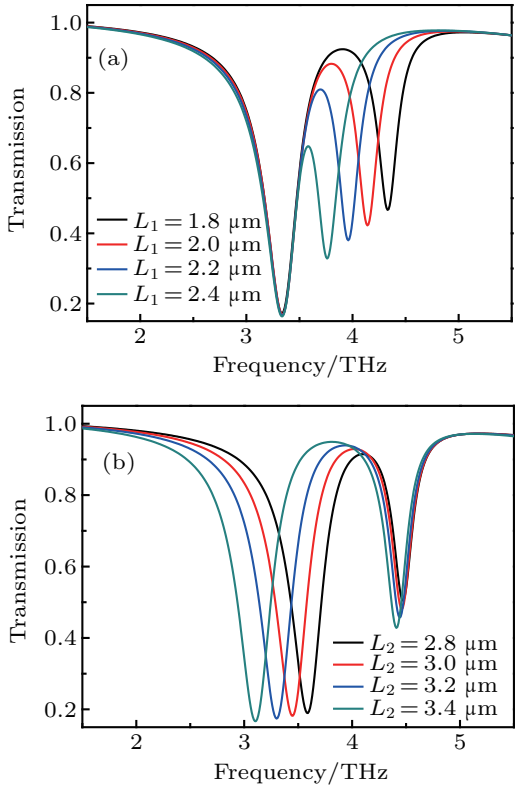


Fig. 5. (a) Plots of spectral response of the graphene-based PIT metamaterial with L_1 values of 1.8 μm, 2.0 μm, 2 2 μm, and 2.4 μm when $L_2 = 3.0$ μm, $d = 0.8$ μm, $E_F = 1.0$ eV. (b) Plots of spectral response of the graphene PIT metamaterial with L_2 values of 2.8 μm, 3.0 μm, 3.2 μm, and 3.4 μm when $L_1 = 1.8$ μm, $d = 0.8$ μm, $E_F = 1.0$ eV.

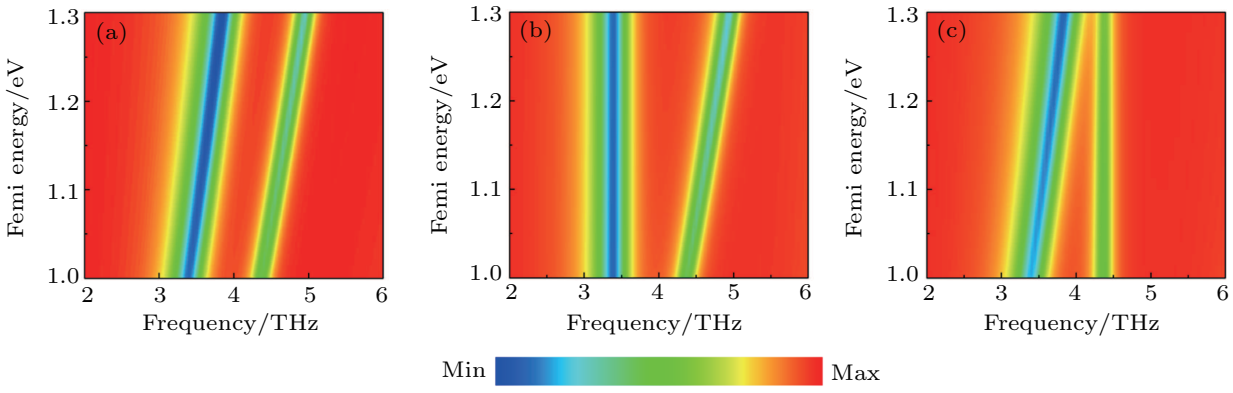


Fig. 6. Contour plots of the transmittance of the structure with different Fermi energies, for (a) graphene PIT structure, (b) short graphene strip L_1, and (c) long graphene strip L_2.

In our simulation, we set $\mu_0 = 10^4$ cm^2·V^{-1}·s^{-1} and calculate the corresponding transmission spectra of the PIT system with μ ranging from $0.3\mu_0$ to $20\mu_0$ in Fig. 7. It can be clearly seen that the transparency window can be effectively tuned with different μ values in Fig. 7(a). The transmission window becomes more obvious with larger μ. It can reach 1.0 with $\mu = 8.0\mu_0$. But the change of the carrier mobility does not affect the position of the transmission dip. Moreover, the transmission of two dips no longer change when the carrier mobility exceeding $10\mu_0$ as shown in Fig. 7(b).

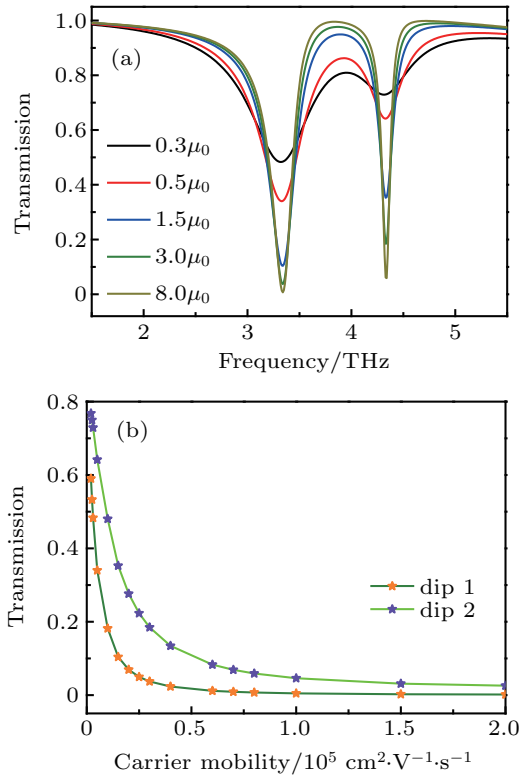


Fig. 7. (a) Transmission spectra of graphene-based PIT metamaterial with different values of μ: $\mu = 0.3\mu$, 0.5μ, 1.5μ. 3.0μ, and 8.0μ. (b) Relationship between transmission and carrier mobility at transmission dips 1 and 2 ($f_1 = 3.33$ THz and $f_2 = 4.33$ THz).

As is well known, a remarkable characteristic of PIT response is phase dispersion in the transparent window region, which leads to slow light effects.[45] Here we introduce the group delay τ_g to describe the slow light capability, which is expressed as[15]

$$\tau_{\mathrm{g}} = -\frac{\mathrm{d}\varphi}{\mathrm{d}\omega}, \tag{8}$$

where φ is the transmission phase shift and ω is the angular frequency, respectively. Figure 8 shows the transmission phase shift and the corresponding group delay at different Fermi energy. It can be seen from Fig. 8(a) that the dispersion gradually increases with Fermi energy increasing, and it also leads the group delay to change from 1.16 ps to 1.25 ps in Fig. 8(b). In addition, we also observe the negative group delay in the nearby region of the transparency window.[46] Therefore, these results demonstrate that our designed structure can achieve the active control of the group delay through Fermi energy.

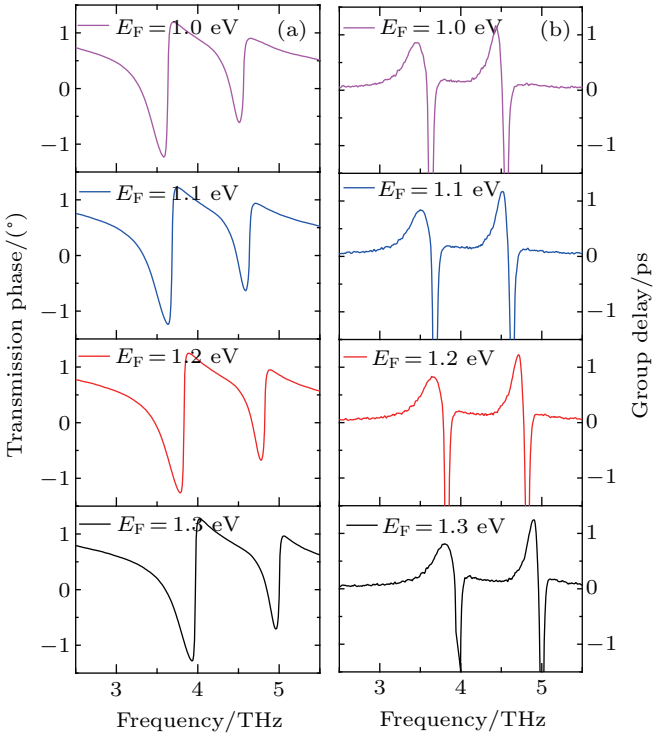


Fig. 8. Optical dispersion characteristics of the PIT structure, showing (a) transmission phase and (b) group delay.

As an application of sensing, the transparency window is sensitive to the variation of a nearby dielectric medium. Namely, small perturbations of the surrounding medium can result in dramatic shifts of a resonance or line shape. Changes due to the presence of molecules close to the cut-out structures in a thin gold film have been detected by Liu *et al.*[8] Fu *et al.* have studied the relationship between transmission peak and substrate refractive index,[14] just as Yu *et al.*'s work.[47] We simulate the changes of transmission spectra at room temperature when the surrounding media are air ($na = 1.000$), perfluorohexane ($np = 1.251$), water ($nw = 1.330$), 60% glucose solution ($ng = 1.439$), and benzene ($nb = 1.501$), respectively. The refractive index of the substrate is 1.5 and remains unchanged throughout the simulation. Figure 9(a) shows the plots of the transmission spectra with different refractive indices of nearby dielectric media above graphene. With our proposed graphene based PIT metamaterial, the transparency window embodies an obvious red-shift with the increase of the nearby dielectric media refractive index and the resonance strength of the PIT window is slightly enhanced. Figure 9(b) shows the relationship between transparency window and refractive index. It is easy to see from Fig. 9(b) that the position of the transparency window is linearly related to the refractive index of the dielectric medium above the structure. It is demonstrated that the graphene based PIT structure may serve as a highly efficient sensor in the THz region. Hence, on the basis of the results and analysis, one can easily control the resonance wavelength by fitting the material with suitable refractive index. This will open a new route for metamaterial applications in sensing chemical and biomedical molecules.

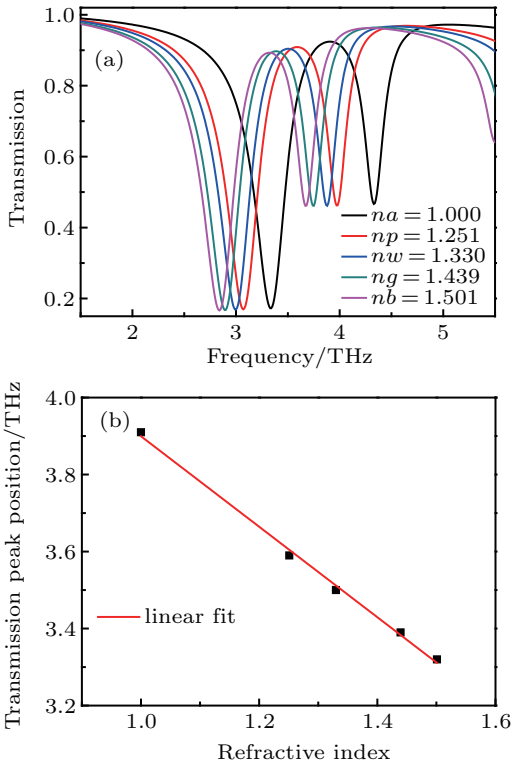


Fig. 9. (a) Transmission spectra of the graphene-based PIT structure at different refractive indices, where $L_1 = 1.8$ μm, $L_2 = 3.0$ μm, $d = 0.8$ μm, $E_F = 1.0$ eV. (b) Relation between resonant PIT peak and refractive index.

4. Conclusions

The optical properties of graphene-based PIT metamaterial which is composed of two horizontal strips attached to continuous vertical wire in THz region are numerically investigated. With the surface current distribution, we can find the distinct PIT window in the graphene metamaterial results from the near-field coupling of two graphene resonators. Such a transmission can also be well fitted with the coupled Lorentz oscillator model. It is noteworthy that the resonance frequency of transparency window can be dynamically tuned by varying the Fermi energy and the carrier mobility of graphene rather than refabricating the nanostructures. The slow light effect can be realized in the PIT structure. In addition, the position of the transmission peak of the proposed structure changes linearly with the refractive index of the nearby dielectric medium. Such a proposed graphene-based PIT system may open up the way for the developing the compact elements of tunable graphene-based photonic devices.

References

[1] Harris S E, Field J and Imamoğlu A 1990 *Phys. Rev. Lett.* **64** 1107
[2] Boller K J, Imamoglu A and Harris S E 1991 *Phys. Rev. Lett.* **66** 2593
[3] Fleischhauer M, Imamoglu A and Marangos J P 2005 *Rev. Mod. Phys.* **77** 633
[4] He J N, Wang J Q, Ding P, Fan C Z, Arnaut L R and Liang E J 2015 *Plasmonics* **10** 1115
[5] Verellen N, Sonnefraud Y, Sobhani H, Hao F, Moshchalkov V V, Dorpe P V, Nordlander P and Stefan A 2009 *Nano Lett.* **9** 1663
[6] Tian Y C, Jia W, Ren P W and Fan C Z 2018 *Chin. Phys. B* **27** 124205
[7] Luk'yanchuk B, Zheludev N I, Maier S A, Halas H J, Nordlander P, Giessen H and Chong C T 2010 *Nat. Mater.* **9** 707
[8] Liu N, Weiss T, Mesch M, Langguth L, Eigenthaler U, Hirscher M, Sönichsen C and Giessen H P 2010 *Nano Lett.* **10** 1103
[9] Yu Z, Che H, Liu J J, Jing X F, Li X J and Hong Z 2017 *Chin. Phys. B* **26** 077804
[10] Zhang Y, Li J, Li H and Yuan P 2013 *Opt. Laser Technol.* **49** 202
[11] Novikova I, Walsworth R L and Xiao Y 2012 *Laser Photon. Rev.* **6** 333
[12] Chen J X, Wang P, Chen C C, Lu Y H, Ming H and Zhan Q W 2011 *Opt. Express* **19** 5970
[13] Safavi-Naeini A H, Alegre T P M, Chan J, Eichenfield M, Winger M, Lin Q, Hill J T, Chang D E and Painter O 2011 *Nature* **472** 69
[14] Fu G L, Zhai X, Li H J, Xia S X and Wang L L 2016 *Plasmonics* **11** 1597
[15] He X J, Yao Y, Yang X Y, Lu G J, Yang W L, Yang Y Q, Wu F M, Yu Z G and Jiang J X 2018 *Opt. Commun.* **410** 206
[16] Tian Y C, Ding P and Fan C Z 2017 *Opt. Eng.* **56** 107106
[17] Shang X J, Zhai X, Li X F, Wang L L, Wang B X and Liu G D 2016 *Plasmonics* **11** 419
[18] Monika D K, Sarma A K, Roy C D and Kumar G 2017 *Opt. Express* **25** 10484
[19] Zhu Y, Hu X Y, Yang H and Gong Q H 2014 *Sci. Rep.* **4** 3752
[20] Zhang S, Genov D A, Wang Y, Liu M and Zhang X 2008 *Phys. Rev. Lett.* **101** 047401
[21] Liu N, Langguth L, Weiss T, Kästel J, Fleischhauer M, Pfau T and Giessen H 2009 *Nat. Mater.* **8** 758
[22] Novoselov K S, Geim A K, Morozov S V, Jiang D, Katsnelson M I, Grigorieva I V, Dubonos S V and Firsov A A 2005 *Nature* **438** 197
[23] Li H J, Wang L L, Liu J Q, Huang Z R, Sun B and Zhai X 2013 *Appl. Phys. Lett.* **103** 211104
[24] Luo X, Qiu T, Lu W, Ni Z 2013 *Mater. Sci. Eng. R* **74** 351
[25] Sensale-Rodriguez B, Yan R, Kelly M M, Fang T, Tahy K, Hwang W S, Jena D, Liu L and Xing H G 2012 *Nat. Commun.* **3** 780
[26] Wang F, Zhang Y, Tian C, Girit C, Zettl A, Crommie M and Shen Y R 2008 *Science* **320** 206
[27] Fei Z, Sn A, Andreev G O, Bao W, McLeod A S, Wagner M, Zhang L M, Zhao Z, Thiemens M, Dominguez G, Fogler M M, Castro Neto A H, Lau C N, Keilmann F and Basov D N 2012 *Nature* **487** 82
[28] Koppens F H L, Chang D E and Garcia de Abajo F J 2011 *Nano Lett.* **11** 3370
[29] Sun C, Si J N, Dong Z W and Deng X X 2016 *Opt. Express* **24** 11466
[30] Shi X, Han D Z, Dai Y Y, Yu Z F, Sun Y, Chen H, Liu X H and Zi J 2013 *Opt. Express* **21** 28438
[31] Nikitin A Y, Guinea F and Martin-Moreno L 2012 *Appl. Phys. Lett.* **101** 151119
[32] Ke S, Wang B, Huang H, Long H, Wang K and Lu P 2015 *Opt. Express* **23** 8888
[33] Falkovsky L A and Pershoguba S S 2007 *Phys. Rev. B* **76** 153410
[34] Jiang J X, Zhang Q F, Ma Q X, Yan S T, Wu F M and He X J 2015 *Opt. Mater. Express* **5** 1962
[35] Novoselov K S, Geim A K, Morozov S V, Jiang D, Zhang Y, Dubonos S V, Grigorieva I V and Firsov A A 2004 *Science* **306** 666
[36] Hao Y F, Bharathi M S, Wang L, Liu Y Y, Chen H, Nie S, Wang X H, Chou H, Tan C, Fallahazad B, Ramanarayan H, Magnuson C W, Tutuc E, Yakobson B I, McCarty K F, Zhang Y W, Kim P, Hone J, Colombo L and Ruoff R 2013 *Science* **342** 720
[37] Zhang S, Genov D A, Wang Y, Liu M and Zhang X 2008 *Phys. Rev. Lett.* **101** 047401
[38] Niu Y, Wang J, Hu Z and Zhang F 2018 *Opt. Commun.* **416** 77
[39] Cheng H, Chen S, Yu P, Duan X, Xie B and Tian J 2013 *Appl. Phys. Lett.* **103** 203112
[40] Artar A, Yanik A A and Altug H 2011 *Nano Lett.* **11** 1685
[41] Shang X J, Zhai X, Li X F, Wang L L, Wang B X and Liu G D 2016 *Plasmonics* **11** 419
[42] Garcia de Abajo J F 2014 *ACS Photonics* **1** 135
[43] Ju L, Geng B, Horng J, Girit C, Martin M, Hao Z, Bechtel H A, Liang X, Zettl A, Shen Y R and Wang F 2011 *Nat. Nanotechnol.* **6** 630
[44] Huang S Y, Song C Y, Zhang G W and Yan H G 2016 *Nanophotonics* **6** 1191
[45] Cao W, Singh R, Zhang C H, Han J G, Tonouchi M and Zhang W L 2013 *Appl. Phys. Lett.* **103** 101106
[46] Zhao Z Y, Song Z Q, Shi W Z and Peng W 2016 *Opt. Mater. Express* **6** 2190
[47] Yu D M, Zhai X, Wang L L, Lin Q, Li H J, Xia S X and Shang X J 2016 *Plasmonics* **11** 1151